International Journal of Thermodynamics (IJoT)
ISSN 1301-9724 / e-ISSN 2146-1511
www.ijoticat.com

Vol. 20 (No. 1), pp. 26-34, 2017
doi: 10.5541/ijot.5000202431
Published online: March 1, 2017

Transient Thermal Stresses of Annulus Elliptical Plate with Mixed-Type Boundary Conditions

Pravin Bhad[1], Vinod Varghese[2], Lalsingh Khalsa[2]

[1]Department of Mathematics, Priyadarshini J.L. College of Engineering, Nagpur, India.
[2]Department of Mathematics, M.G. College, Armori, Gadchiroli, India
E-mail: [1]praash.bhad@gmail.com

Received 28 September 2016, Revised 30 October 2016, Accepted 02 December 2017

Abstract

In this paper, we consider a transient thermal stress investigation into an annulus thin elliptical plate in which edges are fixed and clamped. The realistic problem of the plate is supposed with mixed-type boundary conditions subjected to arbitrary initial temperature on the upper face, and the lower face is kept at zero temperature. Things get further complicated when internal heat generation persists in the object and further becomes unpredictable when sectional heat supply is impacted on the body. The solution to conductivity equation and the corresponding initial and boundary conditions is solved by employing a new integral transform technique. The governing equation for small deflection is found and utilized to preserve the intensities of thermal bending moments and twisting moments, involving the Mathieu and modified functions and their derivatives. It was found that the deflection result nearly agrees with the previously given result. Thus, the numerical results obtained are accurate enough for practical purposes. Conclusions emphasize the importance of better understanding the underlying elliptic structure, improved understanding of its relationship to circular object profile, and better estimates of the thermal effect of the thermoelastic problem.

Keywords: *Elliptical annulus plate; temperature distribution; thermal stresses; Mathieu function; thermal moment.*

1. Introduction

Thermoelastic problems with mixed-type boundary conditions frequently occur in engineering applications. Such examples include the dip-forming process in metallurgy, the surface rewetting during loss-of-coolant accidents, the contact resistance between solids, etc. In the heat conduction analysis of these problems, the conventional integral transform method cannot be applied. We have to rely on the Wiener-Hopf technique or the dual integral/series equation. Due to the complexity of the problem or the existing methodologies, availability of closed-form solutions is limited. Nonetheless, numerical solutions are preferred and prevalent in practice, due to either non-availability or mathematical complexity of the corresponding exact solutions. Rather, limited utilization of analytical solutions should mustn't diminish their merit over numerical ones; since exact solutions, if available, provide an insight into the governing physics of the problem, that is often missing in any numerical solution. Moreover, analyzing closed-form solutions to obtain optimal design options for any particular application of interest is relatively simpler.

Of most recent literature, some authors have undertaken the work on mixed-type boundary conditions, which can be summarised as given below. Han and Hasebe [1] used Green's function of a point heat source for a mechanical mixed boundary value problem of an infinite plane with an arbitrary hole, for which zero-displacement and traction-free boundary conditions are prescribed at its boundary. By employing the mapping technique and complex variable method, an exact solution including a hyper-geometrical function is obtained. In another paper, they [2] derived the Green's function for the bending problem of a thin plate with an elliptical hole under a bending heat source. Naser [3] determined a solution for a non-stationary heat equation in axial-symmetric cylindrical coordinates under mixed discontinuous boundary of the first and second kind conditions, using Laplace transform and separation of variables method used to solve the considered problem which is the dual integral equations method. Helsing [4] formulated an elastic problem with mixed boundary conditions, that is, Dirichlet conditions on parts of the boundary and Neumann conditions and solved on an interior planar domain using an integral equation method. Dang and Mai [5] estimated mixed boundary value problem for a biharmonic equation of the Airy stress function which models a crack problem of a rigid elastic plate using an iterative method. Al Duhaim et al. [6] determined the thermal stress of a mixed boundary value problem in half space using the Jones's modification of the so-called Wiener-Hopf technique. Parnell et al. [7] employed Wiener-Hopf and Cagniard-de Hoop techniques to solve a range of transient thermal mixed boundary value problems in the half space. Nuruddeen and Zaman [8] obtained the analytical solution of transient heat conduction in a solid homogeneous infinite circular cylinder using the Wiener-Hopf technique owing to the mixed nature of the boundary conditions.

It was observed from the previous literature that the thermoelastic problems for an elliptical plate with mixed-type boundary conditions, in which plates are considered to be fixed and clamped, have not been taken into account for the study. Though, bending problems for fixed and clamped elliptical plates under the action of various external forces got wide consideration for practical applications in aircraft structures during the past years. The solution for elliptical thin plates bent by a strong moment placed at the centre of the plate is sought for built-in edges and for fixed, and clamped edges have been investigated by Cheng [9] with the aid of tensor calculus. The expressions for moments,

[1]Corresponding Author

shearing forces and the biharmonic equation for deflection were transformed into elliptic coordinates. Sato [10] used Mathieu functions to study the bending of a clamped as well as simply-supported elliptical plate undergoing the combined action of uniform lateral load over its entire surface and normal in-plane force distributed in its central plane. Most of the studies considered by authors above have examined the bending of an elliptical structural element subjected to the combined action of uniform lateral load and in-plane force treated in terms of the exact analytical method in case of simply supported so as to rotate freely. Bhad et al. [11] investigated the thermoelastic problems on an elliptical plate in which internal heat sources are generated within the solid, with compounded effect due to sectional heating and boundary conditions of the Dirichlet type based on the theory of integral transformations. However, till date, nobody has studied any thermoelastic problem for elliptical plates with boundary conditions as mixed type, in which plates are considered to be fixed and clamped. Based on the thermal small-deflection classical theory, the stresses components are formulated using resultant forces and resultant moments in terms of the elliptical coordinates.

2. Formulation of the Problem

It is assumed that a thin elliptical plate is occupying the space $D:\{(\xi,\eta,z)\in R^3 : a<\xi<b,\ 0<\eta<2\pi,\ 0<z<\ell\}$ under unsteady-state temperature field due to internal heat source within it. The geometry of the plate indicates that an elliptic coordinate system (ξ,η,z) is the most appropriate choices of the reference frame, which are related to the rectangular coordinate system (x,y,z) by reklations $x=c\cosh\xi\cos\eta,\ \ y=c\sinh\xi\sin\eta,\ \ z=z$. The curves $\eta=$ constant represent a family of confocal hyperbolas while the curves $\xi=$ constant constitute a family of confocal ellipses (refer Figure 1). Both sets of curves intersect each other orthogonally at every point in space. The geometry parameters are given as $\xi\in[a,b],\ \ \eta\in[0,2\pi)$ and $z\in(0,\ell)$.

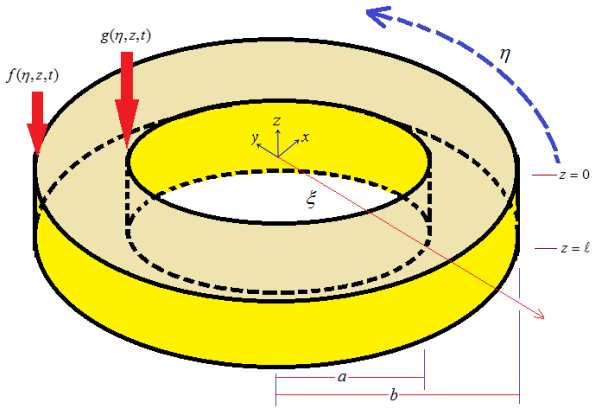

Figure 1. Plate physical configuration.

The heat conduction equation and boundary conditions are given as

$$h^2\left\{\frac{\partial^2\theta}{\partial\xi^2}+\frac{\partial^2\theta}{\partial\eta^2}\right\}+\frac{\partial^2\theta}{\partial z^2}+\frac{Q(\xi,\eta,t)}{\lambda}=\frac{1}{\kappa}\frac{\partial\theta}{\partial t} \tag{1}$$

where $\theta(\xi,\eta,z,t)$ is temperature of the plate at point (ξ,η,z) at t time, λ is the coefficient of thermal conductivity, $Q(\xi,\eta,t)$ represents an energy generation term, $\kappa=\lambda/\rho C$ represents thermal diffusivity in which λ being the thermal conductivity of the material, ρ is the density, C is the calorific capacity, assumed to be constant and

$$h^{-2}=(c^2/2)(\cosh 2\xi-\cos 2\eta). \tag{2}$$

The heat generation term is assumed in the form

$$Q(\xi,\eta,z,t)=Q_0\delta(\xi-a_0)\delta(\eta-2\pi)\delta(z-\ell_0) \tag{3}$$

in which Q_0 characterises the stream of heat, $\delta(\ )$ is the Dirac delta function in which $\xi\neq a_0, a_0\in[a,b]$ and $z\neq\ell_0,\ \ \ell_0\in[0,\ell]$.

The temperature distribution in the elliptical plate is obtained as a solution of the Eq. (1) with the following initial and boundary conditions

$$\theta(\xi,\eta,z,0)=0 \tag{4}$$

$$\frac{\partial\theta}{\partial\xi}(a,\eta,z,t)=f(\eta,z,t) \tag{5}$$

$$\frac{\partial\theta}{\partial\xi}(b,\eta,\ell,t)+\theta(b,\eta,\ell,t)=g(\eta,z,t) \tag{6}$$

$$\theta(\xi,\eta,0,t)=0 \tag{7}$$

$$\theta(\xi,\eta,\ell,t)=0 \tag{8}$$

in which $f(\eta,z,t)$ and $g(\eta,z,t)$ are separate heat supply on the curved surfaces having the boundary conditions of mixed-type.

The most general form of the equation of equilibrium for a plate element is expressed in terms of the partial derivatives of the deflection is found to satisfy the differential equations as

$$D\nabla^4\omega+\nabla^2M_\theta/(1-\upsilon)=0 \tag{9}$$

where D is the stiffness coefficient of the plate and denoted as

$$D=E\ell^3/[12(1-\upsilon^2)] \tag{10}$$

moreover, M_θ is bending of the plate due to change in the temperature and expressed as

$$M_\theta=\alpha E\int_0^\ell z\,\theta\,dz \tag{11}$$

in which ∇^2 denotes the two-dimensional Laplacian operator in (ξ,η), υ denotes Poisson's ratio, α and E denoting coefficient of linear thermal expansion and Young's Modulus of the material of the plate respectively.

Furthermore, the thermal stress components in terms of resultant forces and resultant moments are given [11,12] as

$$\left.\begin{aligned}\sigma_{\xi\xi}&=\frac{1}{\ell}N_\xi+\frac{12z}{\ell^3}M_\xi+\frac{1}{1-\upsilon}\left(\frac{1}{\ell}N_\theta+\frac{12z}{\ell^3}M_\theta-\alpha E\theta\right)\\ \sigma_{\eta\eta}&=\frac{1}{\ell}N_\eta+\frac{12z}{\ell^3}M_\eta+\frac{1}{1-\upsilon}\left(\frac{1}{\ell}N_\theta+\frac{12z}{\ell^3}M_\theta-\alpha E\theta\right)\\ \sigma_{\xi\eta}&=\frac{1}{\ell}N_{\xi\eta}-\frac{12z}{\ell^3}M_{\xi\eta}\end{aligned}\right\} \tag{12}$$

in which components of resultant moments and resultant force are related to the thermal deflection.

The complementary component of resultant forces $(N_{ij},\ i,j=\xi,\eta)$ can be defined as

$$N_{\xi} = N_{\eta} = N_{\xi\eta} = 0 \tag{13}$$

moreover, the thermally induced resultant force is

$$N_{\theta} = \alpha E \int_0^{\ell} \theta \, dz \tag{14}$$

The complement components of resultant bending moments can be defined as

$$\left.\begin{aligned}
M_{\xi} &= \frac{-2D}{c^2(\cosh 2\xi - \cos 2\eta)} \left\{ \begin{aligned} &\left[\frac{\partial^2 \omega}{\partial \xi^2} - \frac{(1-\upsilon)\sinh 2\xi}{(\cosh 2\xi - \cos 2\eta)} \frac{\partial \omega}{\partial \xi} \right] \\ &+ \left[\upsilon \frac{\partial^2 \omega}{\partial \eta^2} + \frac{(1-\upsilon)\sin 2\eta}{(\cosh 2\xi - \cos 2\eta)} \frac{\partial \omega}{\partial \eta} \right] \end{aligned} \right\} - M_{\theta} \\
M_{\eta} &= \frac{-2D}{c^2(\cosh 2\xi - \cos 2\eta)} \left\{ \begin{aligned} &\left[\upsilon \frac{\partial^2 \omega}{\partial \xi^2} + \frac{(1-\upsilon)\sinh 2\xi}{(\cosh 2\xi - \cos 2\eta)} \frac{\partial \omega}{\partial \xi} \right] \\ &+ \left[\frac{\partial^2 \omega}{\partial \eta^2} - \frac{(1-\upsilon)\sin 2\eta}{(\cosh 2\xi - \cos 2\eta)} \frac{\partial \omega}{\partial \eta} \right] \end{aligned} \right\} - M_{\theta} \\
M_{\xi\eta} &= \frac{2D(1-\upsilon)}{c^2(\cosh 2\xi - \cos 2\eta)} \left\{ \begin{aligned} &\frac{\partial \omega}{\partial \xi} \sin 2\eta + \frac{\partial \omega}{\partial \eta} \sinh 2\xi \\ &- \frac{\partial^2 \omega}{\partial \xi \partial \eta} (\cosh 2\xi - \cos 2\eta) \end{aligned} \right\}
\end{aligned}\right\} \tag{15}$$

In order to complete the formulation of the problem, it is necessary to introduce suitable boundary conditions. The plate edge is assumed to be fixed and clamped, that is

$$\omega(\xi,\eta,0) = 0,\ \omega(a,\eta,t) = \frac{\partial \omega(b,\eta,t)}{\partial \xi} = 0 \tag{16}$$

The Eqs. (1)-(16) constitute the mathematical formulation of the problem under consideration.

3. Solution to the Problem

To solve fundamental differential Eq. (1), Firstly we introduce the new integral transformation of order *n* and *m* over the variable ξ and η as

$$\begin{aligned}
\overline{\vartheta}(q_{2n,m}) = \int_a^b \int_0^{2\pi} \vartheta(\xi,\eta)(\cosh 2\xi - \cos 2\eta) \\
\times M_{2n,m}(k,\xi,q_{2n,m}) ce_{2n}(\eta,q_{2n,m})\, d\xi\, d\eta
\end{aligned} \tag{17}$$

The inversion theorem of (17) is

$$\begin{aligned}
\vartheta(\xi,\eta) = \sum_{n=0}^{\infty}\sum_{m=1}^{\infty} \overline{\vartheta}(q_{n,m}) M_{2n,m}(k,\xi,\eta,q_{n,m}) \\
\times ce_{2n}(\eta,q_{2n,m}) / C_{2n,m}
\end{aligned} \tag{18}$$

where, the kernel is given as

$$\begin{aligned}
M_{2n,m}(k,\xi,\eta,q_{n,m}) = \{ [fey_{2n}(a,q_{2n,m}) + \mathrm{B}_{2n}(k,b,q_{2n,m})] \\
Ce_{2n}(\xi,q_{2n,m}) - [Ce_{2n}(a,q_{2n,m}) \\
+ \mathrm{A}_{2n}(k,b,q_{2n,m})]\, fey_{2n}(\xi,q_{2n,m})\}
\end{aligned}$$

in which $q_{2n,m}$ is a root of the transcendental equation

$$Ce_{2n}(a,q_{2n,m})\mathrm{B}_{2n}(k,b,q_{2n,m}) - fey_{2n}(a,q_{2n,m})\mathrm{A}_{2n}(k,b,q_{2n,m}) = 0,$$

$$\mathrm{A}_{2n}(k,b,q_{2n,m}) = Ce_{2n}(b,q_{2n,m}) + k\, Ce'_{2n}(b,q_{2n,m}),$$

$$\mathrm{B}_{2n}(k,b,q_{2n,m}) = fey_{2n}(b,q_{2n,m}) + k\, fey'_{2n}(b,q_{2n,m}),$$

$$C_{2n,m} = \pi \int_a^b (\cosh 2\xi - \Theta_{2n,m}) \mathrm{M}^2_{2n,m}(\xi, q_{2n,m})\, d\xi$$

and operational property as

$$\begin{aligned}
\int_a^b \int_0^{2\pi} \left(\frac{\partial^2 f}{\partial \xi^2} + \frac{\partial^2 f}{\partial \eta^2} \right) M_{2n,m}(k,\xi,\eta,q_{2n,m})\, ce_{2n}(\eta,q_{2n,m})\, d\xi\, d\eta \\
= -2q_{2n,m} \bar{f} + \left(\ell \frac{\partial f}{\partial \xi} + f \right)\Big|_{\xi=b} M_{2n,m}(k,b,\eta,\ell,q_{2n,m}) \\
- \left(\frac{\partial f}{\partial \xi} \right)\Big|_{\xi=a} M'_{2n,m}(k,a,\eta,\ell,q_{2n,m})
\end{aligned} \tag{19}$$

The kernel of above transform is indicated in elliptical function, and it removes the variable ξ and η from the differential equation defined in (1) for the mixed-type boundary conditions given in Eqs. (5) and (6). On applying new integral transform in Eq. (17) to the differential Eq. (1), and taking the property (19) into account under the conditions (5) and (6), the differential equation for the temperature $\theta(\xi,\eta,z,t)$ is reduced to

$$\frac{\partial^2 \overline{\theta}}{\partial z^2} - \frac{4q_{2n,m}}{c^2} \overline{\theta} + \Omega(z,t) + \frac{\overline{Q}}{\lambda} = \frac{1}{\kappa} \frac{\partial \overline{\theta}}{\partial t} \tag{20}$$

$$\Omega(z,t) = 2\alpha\pi\, A_0^{(2n)} \{ M_{2n,m}(b,q_{2n,m})\, g(z,t) - M'_{2n,m}(a,q_{2n,m})\, f(z,t) \}$$

Then, applying Fourier finite sine transform to the Eq. (20) moreover, taking into account the boundary conditions (7) and (8), the differential equation for $\overline{\theta}(q_{2n,m},z,t)$ is transformed into

$$\frac{\partial \overline{\theta}^*}{\partial t} + \alpha^2_{2n,m} \overline{\theta}^* = \Omega^*(\beta_p,t) + \overline{Q}^* \tag{21}$$

where

$$\alpha_{2n,m} = \kappa(4q_{2n,m}/c^2 + {\beta_p}^2),$$

and β_p is a positive root of the transcendental equation $\sin(\beta_p) = 0$, $\beta_p = m\pi/\ell$.

Thus, temperature solution in the transformed domain reduces to

$$\overline{\theta}^*(q_{2n,m},\beta_p,t) = \int_0^t \exp[-\alpha_{2n,m}(t-\tau)][\,\Omega^*(\beta_p,t) + \overline{\theta}^*]\, d\tau \tag{22}$$

Finally, using the inversion of the Fourier finite sine transform and the inversion theorem (18), we obtain the solution as

$$\begin{aligned}
\theta(\xi,\eta,z,t) = \frac{2}{\ell} \sum_{n=0}^{\infty}\sum_{m=1}^{\infty} \left\{ \sum_{p=0}^{\infty} \sin(\beta_p z) [\int_0^t \exp[-\alpha_{2n,m}(t-\tau)] \right. \\
\left. \times [\,\Omega^*(\beta_p,t) + \overline{\theta}^*]\, d\tau \right\} M_{2n,m}(\xi,k,q_{2n,m}) \\
\times ce_{2n}(\eta,q_{2n,m}) / C_{2n,m}
\end{aligned} \tag{23}$$

The above function is given in Eq. (23) represents the temperature at every instance and at all points of the elliptical annulus of finite height under the influence of mixed-type boundary conditions. On substituting Eq. (23) in (9), one obtains the thermal moment as

$$\begin{aligned}
M_{\theta}(\xi,\eta,t) = \frac{2\alpha E}{\ell} \sum_{n=0}^{\infty}\sum_{m=1}^{\infty} \left\{ \sum_{p=0}^{\infty} [\sin(\beta_p) - \beta_p \cos(\beta_p \ell)] \right. \\
\left. \times \int_0^t \exp[-\alpha_{2n,m}(t-\tau)][\,\Omega^*(\beta_p,t) + \overline{\theta}^*]\, d\tau \right\} \\
\times M_{2n,m}(\xi,k,q_{2n,m})\, ce_{2n}(\eta,q_{2n,m}) / C_{2n,m}\, \beta_p^2
\end{aligned} \tag{24}$$

Using Eq. (23) into Eq. (14), one obtains

$$N_\theta(\xi,\eta,t)=\frac{2\alpha E}{\ell}\sum_{n=0}^{\infty}\sum_{m=1}^{\infty}\left\{\sum_{p=0}^{\infty}[1-\cos(\beta_p\,\ell)]\right.$$
$$\times\left.\int_0^t\exp[-\alpha_{2n,m}(t-\tau)][\Omega^*(\beta_p,t)+\bar{\theta}^*]\,d\tau\right\}$$
$$\times M_{2n,m}(\xi,k,q_{2n,m})\,ce_{2n}(\eta,q_{2n,m})/C_{2n,m}\,\beta_p \tag{25}$$

Using Eq. (24) into Eq. (9) satisfying boundary conditions (16), we obtain the expression for thermal deflection as

$$\omega(\xi,\eta,t)=\frac{\alpha c^2 E}{2D(1-\upsilon)}\sum_{n=0}^{\infty}\sum_{m=1}^{\infty}\left\{\sum_{p=0}^{\infty}[\sin(\beta_p)-\beta_p\cos(\beta_p\,\ell)]\right.$$
$$\times\left.\int_0^t\exp[-\alpha_{2n,m}(t-\tau)][\Omega^*(\beta_p,t)+\bar{\theta}^*]\,d\tau\right\}Z_{2n,m}$$
$$\times M'_{2n,m}(a,k,q_{2n,m})\,ce_{2n}(\eta,q_{2n,m})\{a\,Z_{2n,m}$$
$$-\xi[Z_{2n,m}+M_{2n,m}(\xi,k,q_{2n,m})+M_{2n,m}(a,k,q_{2n,m})]\}$$
$$/(a\,q_{2n,m}\,C_{2n,m}\,\beta_p^2) \tag{26}$$

$$Z_{n,m}=M_{2n,m}(a,k,q_{2n,m})-M_{2n,m}(b,k,q_{2n,m})-b\,M'_{2n,m}(a,k,q_{2n,m})$$

Substituting Eqs. (24) and (26) in Eq. (15), one obtains the resultant moment as

$$M_\xi=-\alpha E\ell\sum_{n=0}^{\infty}\sum_{m=1}^{\infty}\left\{\sum_{p=0}^{\infty}[\sin(\beta_p)-\beta_p\cos(\beta_p\,\ell)]\right.$$
$$\times\left.\int_0^t\exp[-\alpha_{2n,m}(t-\tau)][\Omega^*(\beta_p,t)+\bar{\theta}^*]\,d\tau\right\}$$
$$\times\left\langle\frac{ce_{2n}(\eta,q_{2n,m})M_{2n,m}(\xi,k,q_{2n,m})}{(1-\upsilon)\beta_p^2}\right.$$
$$+\frac{M'_{2n,m}(a,k,q_{2n,m})}{\psi_{n,m}\,Z_{2n,m}(1-\upsilon)(-\cos 2\eta+\cosh 2\xi)^2}$$
$$\times[a\,Z_{2n,m}-\xi(Z_{2n,m}+M_{2n,m}(\xi,k,q_{2n,m})$$
$$+M_{2n,m}(a,k,q_{2n,m}))][(1-\upsilon)\sin(2\eta)$$
$$\times ce'_{2n}(\eta,q_{2n,m})+(\cosh(2\xi)-\cos(2\eta))\,\upsilon\,ce''_{2n}(\eta,q_{2n,m})]$$
$$+\sinh 2\xi(1-\upsilon)ce_{2n}(\eta,q_{2n,m})[Z_{2n,m}+M_{2n,m}(\xi,k,q_{2n,m})$$
$$+\xi M'_{2n,m}(\xi,k,q_{2n,m})-M_{2n,m}(a,k,q_{2n,m})]$$
$$-ce_{2n}(\eta,q_{2n,m})[(-\cos 2\eta+\cosh 2\xi)$$
$$\times(\xi M''_{2n,m}(\xi,k,q_{2n,m})+2M'_{2n,m}(\xi,k,q_{2n,m})]\left.\right\rangle \tag{27}$$

$$M_\eta=\alpha E\ell\sum_{n=0}^{\infty}\sum_{m=1}^{\infty}\left\{\sum_{p=0}^{\infty}[\beta_p\cos(\beta_p\,\ell)-\sin(\beta_p)]\right.$$
$$\times\left.\int_0^t\exp[-\alpha_{2n,m}(t-\tau)][\Omega^*(\beta_p,t)+\bar{\theta}^*]\,d\tau\right\}$$
$$\times\left\langle\frac{ce_{2n}(\eta,q_{2n,m})M_{2n,m}(\xi,k,q_{2n,m})}{(1-\nu)\beta_p^2}\right.$$
$$+\frac{M'_{2n,m}(a,k,q_{2n,m})}{\psi_{2n,m}Z_{2n,m}(1-\nu)(-\cos 2\eta+\cosh 2\xi)^2}$$
$$\times[a\,Z_{2n,m}-\xi\,Z_{2n,m}-\xi(M_{2n,m}(\xi,k,q_{2n,m})$$
$$-M_{2n,m}(a,k,q_{2n,m}))][(\cos 2\eta-\cosh 2\xi)\,ce''_{2n}(\eta,q_{2n,m})$$
$$-(1-\upsilon)\sin 2\eta\,ce'_{2n}(\eta,q_{2n,m})]-\sinh 2\xi(1-\upsilon)$$
$$\times ce_{2n}(\eta,q_{2n,m})[Z_{2n,m}+M_{2n,m}(\xi,k,q_{2n,m})$$
$$+\xi M'_{2n,m}(\xi,k,q_{2n,m})[Z_{2n,m}+M_{2n,m}(\xi,k,q_{2n,m})$$
$$-M_{2n,m}(a,k,q_{2n,m})]-\upsilon\,ce_{2n}(\eta,q_{2n,m})[(-\cos 2\eta+\cosh 2\xi)$$
$$\times(\xi M''_{2n,m}(\xi,k,q_{2n,m})+2M'_{2n,m}(\xi,k,q_{2n,m})]\left.\right\rangle \tag{28}$$

$$M_{\xi\eta}=-\alpha E\ell(1-\upsilon)\sum_{n=0}^{\infty}\sum_{m=1}^{\infty}\left\{\sum_{p=0}^{\infty}[\beta_p\cos(\beta_p\,\ell)-\sin(\beta_p)]\right.$$
$$\times\left.\int_0^t\exp[-\alpha_{2n,m}(t-\tau)][\Omega^*(\beta_p,t)+\bar{\theta}^*]\,d\tau\right\}$$
$$\times\left(\frac{M'_{2n,m}(a,k,q_{2n,m})}{\psi_{n,m}\,Z_{2n,m}(-\cos 2\eta+\cosh 2\xi)}\right)$$
$$\times\left\langle\sinh(2\xi)\,ce'_{2n}(\eta,q_{2n,m})[a\,Z_{2n,m}-\xi\,Z_{2n,m}\right.$$
$$-\xi(M_{2n,m}(\xi,k,q_{2n,m})-M_{2n,m}(a,k,q_{2n,m})]$$
$$+[Z_{2n,m}+M_{2n,m}(\xi,k,q_{2n,m})+\xi M'_{2n,m}(\xi,k,q_{2n,m})$$
$$-M_{2n,m}(a,k,q_{2n,m})][(\cosh 2\xi-\cos 2\eta)ce'_{2n}(\eta,q_{2n,m})$$
$$\left.-ce_{2n}(\eta,q_{2n,m})\sin 2\eta]\right\rangle \tag{29}$$

$$\psi_{n,m}=(1-\upsilon)\beta_p^2 a\,q_{2n,m}D_{2n,m}$$

Using Eqs. (24)-(29) in Eq. (12), we derive stresses as

$$\sigma_{\xi\xi}=\frac{12\alpha E}{\ell^3}\sum_{n=0}^{\infty}\sum_{m=1}^{\infty}\left\{\sum_{p=0}^{\infty}z[\beta_p\cos(\beta_p\,\ell)-\sin(\beta_p)]\right.$$
$$\times\left.\int_0^t\exp[-\alpha_{2n,m}(t-\tau)][\Omega^*(\beta_p,t)+\bar{\theta}^*]\,d\tau\right\}$$
$$\times\left\langle\frac{ce_{2n}(\eta,q_{2n,m})M_{2n,m}(\xi,k,q_{2n,m})}{(1-\upsilon)\beta_p^2}\right.$$
$$+\frac{M'_{2n,m}(a,k,q_{2n,m})}{\psi_{n,m}\,Z_{2n,m}(1-\upsilon)(-\cos(2\eta)+\cosh(2\xi))^2}$$
$$\times[a\,Z_{2n,m}-\xi(Z_{2n,m}+M_{2n,m}(\xi,k,q_{2n,m})$$
$$+M_{2n,m}(a,k,q_{2n,m}))][(1-\upsilon)\sin(2\eta)$$
$$\times ce'_{2n}(\eta,q_{2n,m})+(\cosh 2\xi-\cos 2\eta)\,\upsilon$$
$$\times ce''_{2n}(\eta,q_{2n,m})]+\sinh(2\xi)(1-\upsilon)ce_{2n}(\eta,q_{2n,m})$$
$$\times[Z_{2n,m}+M_{2n,m}(\xi,k,q_{2n,m})+\xi M'_{2n,m}(\xi,k,q_{2n,m})$$
$$-M_{2n,m}(a,k,q_{2n,m})]-ce_{2n}(\eta,q_{2n,m})$$
$$\times[(-\cos(2\eta)+\cosh(2\xi))(\xi M''_{2n,m}(\xi,k,q_{2n,m})$$
$$+2M'_{2n,m}(\xi,k,q_{2n,m})]\left.\right\rangle+\frac{\bar{\theta}^*M_{2n,m}(\xi,k,q_{2n,m})}{6\beta_\ell^2D_{2n,m}(1-\upsilon)}$$
$$\{\beta_\ell L(1-\cos(\beta_\ell\ell))+12z[\sin(\beta_\ell)-\beta_\ell\cos(\beta_\ell\ell)]$$
$$\left.-\ell^2\beta_\ell^2\sin(\beta_\ell z)\}ce_{2n}(\eta,q_{2n,m})\right\} \tag{30}$$

$$\sigma_{\eta\eta}=\frac{12\alpha E}{\ell^3}\sum_{n=0}^{\infty}\sum_{m=1}^{\infty}\left\{\sum_{p=0}^{\infty}z[\beta_p\cos(\beta_p\,\ell)-\sin(\beta_p)]\right.$$
$$\times\left.\int_0^t\exp[-\alpha_{2n,m}(t-\tau)][\Omega^*(\beta_p,t)+\bar{\theta}^*]\,d\tau\right\}$$
$$\times\left\langle\frac{ce_{2n}(\eta,q_{2n,m})M_{2n,m}(\xi,k,q_{2n,m})}{(1-\upsilon)\beta_p^2}\right.$$
$$+\frac{M'_{2n,m}(a,k,q_{2n,m})}{\psi_{2n,m}\,Z_{2n,m}(1-\upsilon)(-\cos(2\eta)+\cosh(2\xi))^2}[a\,Z_{2n,m}$$
$$-\xi\,Z_{2n,m}-\xi(M_{2n,m}(\xi,k,q_{2n,m})-M_{2n,m}(a,k,q_{2n,m}))]$$
$$\times[(\cos(2\eta)-\cosh(2\xi))ce_{2n}(\eta,q_{2n,m})ce''_{2n}(\eta,q_{2n,m})$$
$$-(1-\upsilon)\sin 2\eta\,ce'_{2n}(\eta,q_{2n,m})]-\sinh(2\xi)(1-\upsilon)[Z_{2n,m}$$
$$+M_{2n,m}(\xi,k,q_{2n,m})+\xi M'_{2n,m}(\xi,k,q_{2n,m})$$
$$-M_{2n,m}(a,k,q_{2n,m})]-\upsilon\,ce_{2n}(\eta,q_{2n,m})[(-\cos(2\eta)$$
$$+\cosh(2\xi))(\xi M''_{2n,m}(\xi,k,q_{2n,m})+2M'_{2n,m}(\xi,k,q_{2n,m})]\left.\right\rangle$$
$$+\frac{\bar{\theta}^*M_{2n,m}(\xi,k,q_{2n,m})}{6\beta_p^2D_{2n,m}(1-\upsilon)}\{\beta_p\ell(1-\cos(\beta_p\ell))+12z[\sin(\beta_p)$$
$$\left.-\beta_p\cos(\beta_p\ell)]-\ell^2\beta_p^2\sin(\beta_p z)\}ce_{2n}(\eta,q_{2n,m})\right\} \tag{31}$$

$$\sigma_{\xi\eta} = \frac{12\alpha(1-\upsilon)E}{\ell^3}\sum_{n=0}^{\infty}\sum_{m=1}^{\infty}\left\{\sum_{p=0}^{\infty} z[\beta_p\cos(\beta_p\,\ell)-\sin(\beta_p)] \times\int_0^t \exp[-\alpha_{2n,m}(t-\tau)][\Omega^*(\beta_p,t)+\bar{\theta}^*]d\tau\right\} \times\frac{M'_{2n,m}(a,k,q_{2n,m})}{\psi_{n,m}\,Z_{2n,m}(-\cos 2\eta+\cosh 2\xi)}\Big\langle \sinh(2\xi)\,ce'_{2n}(\eta,q_{2n,m}) \times[a\,Z_{2n,m}-\xi\,Z_{2n,m}-\xi(M_{2n,m}(\xi,k,q_{2n,m}) - M_{2n,m}(a,k,q_{2n,m})]+[Z_{2n,m}+M_{2n,m}(\xi,k,q_{2n,m}) + \xi\,M'_{2n,m}(\xi,k,q_{2n,m})-M_{2n,m}(a,k,q_{2n,m})] \times[(\cosh 2\xi-\cos 2\eta) \times ce'_{2n}(\eta,q_{2n,m})-ce_{2n}(\eta,q_{2n,m})\sin(2\eta)]\Big\rangle \tag{32}$$

4. Transition to Annulus Circular Plate

When the elliptical annulus plate tends degenerates into a circular annulus plate with the thickness $\ell\to 0$, internal radius a, and outer radius $b\to\infty$, occupying the space $D'=\{(x,y,z)\in R^3 : a\le(x^2+y^2)^{1/2}\le b,\ z=\ell\}$, where $r=(x^2+y^2)^{1/2}$, in such a way that $h\exp(\xi)/2\to r$, $h\exp(a)/2\to a$, and $h\exp(b)/2\to b$ [14] and taking θ independent of η.

For that we take,

$n=0,\ q\to 0,\ e\to 0,\ \cosh 2\xi\,d\xi\to 2rh^2dr,\ A_2^{(0)}\to 0,$

$A_0^{(0)}\to 1/\sqrt{2},\ \lambda_{0,m}^2\to\alpha_m^2,\ ce_0(\eta,q_{0,m})\to 1/\sqrt{2},$

$ce_0(\xi,q_{0,m})\to J_0(\alpha_m r),\ Fey_0(\xi_0,q_{0,m})\to Y_0(\alpha_m r),$

$\alpha_{2n,m}=\kappa\,(4q_{2n,m}/c^2+\beta_p^2)\to\kappa\,(4\alpha_m/c^2+\beta_p^2)=\alpha_m,$

$\alpha_m(=\alpha_{0,m})$ are the roots of

$$J_0(k_1,\alpha_a)Y_0(k_2,\alpha_b)-J_0(k_2,\alpha_b)Y_0(k_2,\alpha_a)=0 \tag{33}$$

$$\left.\begin{aligned} J_0(k_j,\alpha_i r)&=J_0(\alpha_i r)+k_j J_0'(\alpha_i r)\\ Y_0(k_j,\alpha_i r)&=Y_0(\alpha_i r)+k_j Y_0'(\alpha_i r)\end{aligned}\right\}\ j=1,2,\ i=a,b \tag{34}$$

$$\left.\begin{aligned} &Ce_0(k_1,\xi,\eta,q_{0,m})\to Ce_0(k_1,r\alpha_m)\\ &Fey_0(k_1,\xi,\eta,q_{0,m})\to Fey_0(k_1,r\alpha_m)\\ &S_{0,m}(k_1,k_2,\xi,\eta,q_{0,m})\to S_{0,m}(k_1,k_2,r\alpha_m)\\ &\qquad\qquad (=S_m(k_1,k_2,r\alpha_m))\end{aligned}\right\} \tag{35}$$

Eq. (21) degenerates into temperature distribution in hollow circular disc

$$\theta(r,z,t)=\frac{2}{\ell}\sum_{n=0}^{\infty}\sum_{m=1}^{\infty}\left\{\sum_{p=0}^{\infty}\sin(\beta_p z)[\int_0^t\exp[-\alpha_{2n,m}(t-\tau)] \times[\Omega^*(\beta_p,t)+\bar{\theta}^*]d\tau]\right\}S_m(k_1,k_2,r\alpha_m)\,J_0(r\alpha_m)/N_m \tag{36}$$

in which

$N_m=\int_a^b r\,S_m^2(k_1,k_2,r\alpha_m)\,dr,$

moreover, the kernel can be defined as

$$S_m(k_1,k_2,r\alpha_m)=J_0(r\alpha_m)\,[Y_0(k_1,a\alpha_m)+Y_0(k_2,b\alpha_m)] -Y_0(r\alpha_m)\,[J_0(k_1,a\alpha_m)+J_0(k_2,b\alpha_m)] \tag{37}$$

in which $J_0(r\alpha_m)$ and $Y_0(r\alpha_m)$ are Bessel's function of the first kind and second kind respectively.

The results above agree with the results [13].

5. Numerical Results, Discussion and Remarks

For the sake of simplicity of calculation, we introduce the following dimensionless values

$$\left.\begin{aligned} &\bar{\xi}=\xi/b,\ \bar{a}=a/b,\ \bar{b}=b/b,\ \bar{z}=z/b,\ \bar{\ell}=\ell/b,\\ &e=c/b,\ \tau=\kappa t/b^2,\bar{\theta}=\theta/\theta_0,\varpi=\omega/E\alpha_t\theta_0 b,\\ &\bar{\sigma}_{ij}=\sigma_{ij}/E\alpha_t\theta_0\ \ (i,j=\xi,\eta),\end{aligned}\right\} \tag{38}$$

Substituting the value of Eq. (33) in Eqs. (26)-(32), we obtained the expressions for the temperature and stresses, respectively for our numerical discussion. The numerical computations have been carried out for Aluminum metal with parameter a = 1 cm, b = 2 cm, ℓ = 0.128 cm, $f(z,t)=g(z,t)=\delta(z-\ell_0)\delta(t)$, $z\neq\ell_0$, $z\in[0,\ell]$, Modulus of Elasticity $E = 6.9\times10^6$ N/cm^2, Shear modulus $G = 2.7\times10^6$ N/cm^2, Poisson ratioυ = 0.281, Thermal expansion coefficient, $\alpha = 25.5\times10^{-6}$ cm/cm-^{0}C, Thermal diffusivity κ = 0.86 cm^2/sec, Thermal conductivity λ = 0.48 calsec^{-1}/cm^{0}C with $\alpha_{2n,m}=0.0986$, 0.3947, 0.8882, 1.5791, 2.4674, 3.5530, 4.8361, 6.3165, 7.9943, 9.8696, 11.9422, 14.2122, 16.6796, 19.3444, 22.2066, 25.2661, 28.5231, 31.9775, 35.6292, 39.4784 are the positive & real roots of the transcendental equation. In order to examine the influence of heating on the plate, we performed the numerical calculation for all variables, and numerical calculations are depicted in the following figures with the help of MATHEMATICA software. Figures 2–7 illustrate the numerical results of temperature distribution, bending moments, thermal deflection, and stresses of the elliptical plate due to internal heat generation within the solid, under thermal mixed-type boundary conditions. Figure 2(a) indicates the temperature distribution along the $\bar{\xi}$-direction of the plate. The maximum value of temperature magnitude occurs at the outer face due to additional heat supply, and internal heat energy throughout the body. The distribution of the temperature gradient at each instance decreases towards inner face along the radial direction.

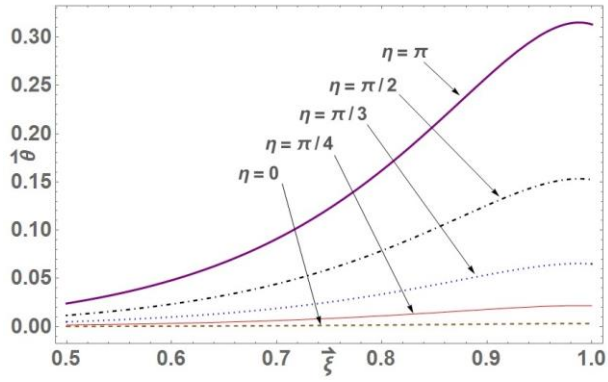

Figure 2(a) Distribution of the dimensionless temperature along $\bar{\xi}$ for the different values of η.

Figure 2(b) illustrates temperature profile along the angular direction for various values of *z*. At the center of the core, temperature fluctuation is high compared to the inner and outer edge. This appearance may be due to more accumulation of heat energy, and hence thermal expansion is more giving high tensile force. Vis-à-vis, similar characteristic, was found during axis change in the graph as shown in Figure 2(c). As expected in Figure 2(d), with an increase of time in small value, the temperature increases

along a radial direction towards the outer edge. This increase could be due to thermal deformation occurring with additional sectional heat.

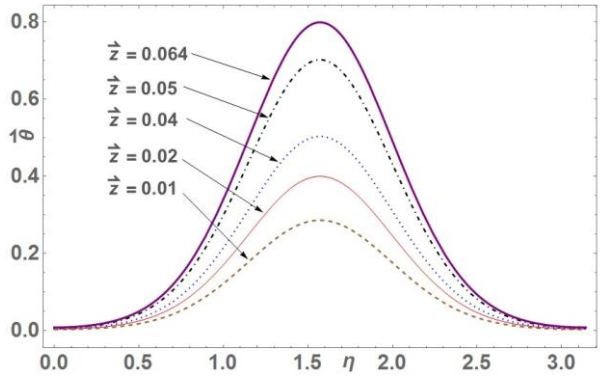

Figure 2(b) Distribution of the dimensionless temperature along η the various values of $\bar{z}$.

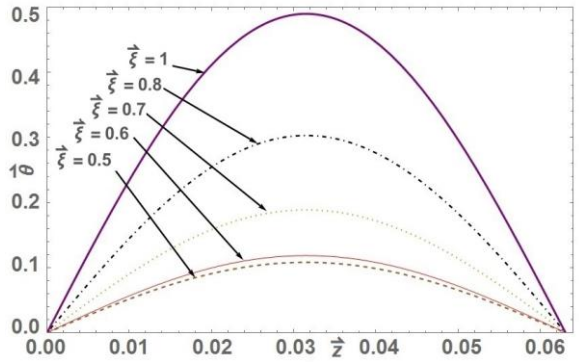

Figure 2(c) Temperature distribution along $\bar{z}$ for the different dimensionless values of $\bar{\xi}$.

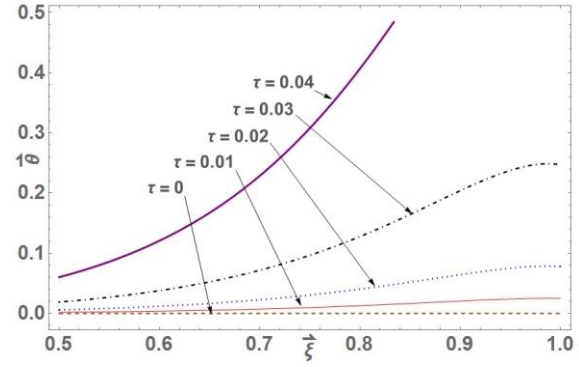

Figure 2(d) Temperature distribution along $\bar{\xi}$ for the different dimensionless values of τ.

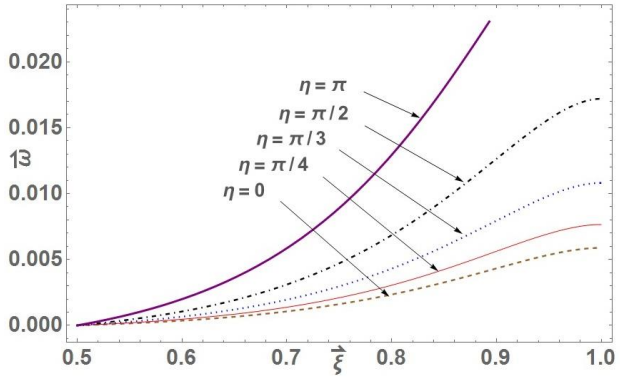

Figure 3(a) Dimensionless thermal deflection along $\bar{\xi}$ for the different values of η.

Figure 3(a) illustrates thermal deflection along the radial direction for different angles which increase with an increase in angular degree towards the outer edge. Whereas it also agrees on Eq. (16), which claims $\omega(a,\eta,t)=0$. In Figure 3(b) thermal deflection is higher at the center of the plate compared to the inner and outer edge of the plate and it may be due to accumulation of energy. Figure 3(c) defection increases along the radial direction for different values of time. It was observed that this graph satisfies Eq. (16) showing $\omega(\xi,\eta,0)=0$. It may be due to more exposure towards heat sources at the outer edge, and hence thermal expansion is more giving high tensile force. Figure 3(d) indicates that the $M_{\xi\xi}$, $M_{\eta\eta}$ and $M_{\xi\eta}$ approaches near to each other towards the centre of the elliptical plate. The residual bending moments are maximum for $M_{\xi\xi}$ and $M_{\eta\eta}$, whereas $M_{\xi\eta}$ is minimum at the outer edge.

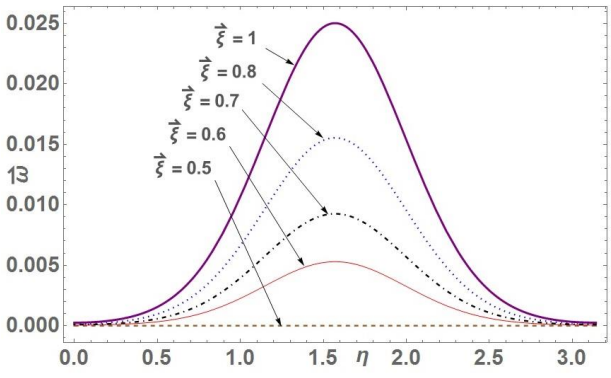

Figure 3(b) Thermal deflection along $\bar{\xi}$ for the different dimensionless values of η.

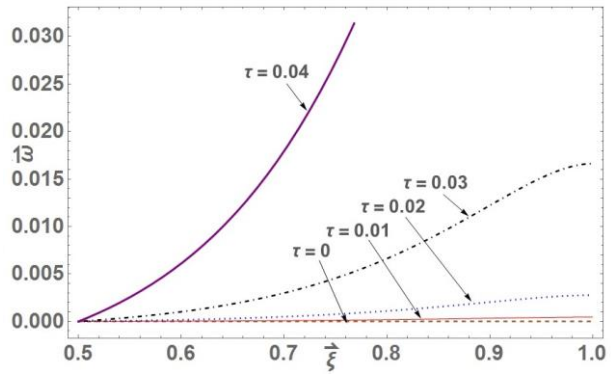

Figure 3(c) Dimensionless thermal deflection along $\bar{\xi}$ for the different values of τ.

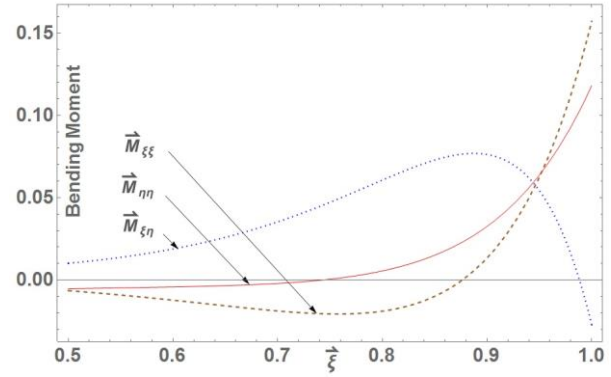

Figure 3(d) Thermally induced bending moments along $\bar{\xi}$.

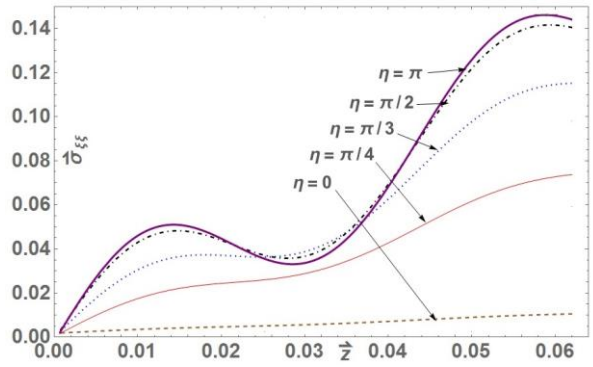

Figure 4(a) Dimensionless Radial stress along $\bar{z}$ for the different values of η.

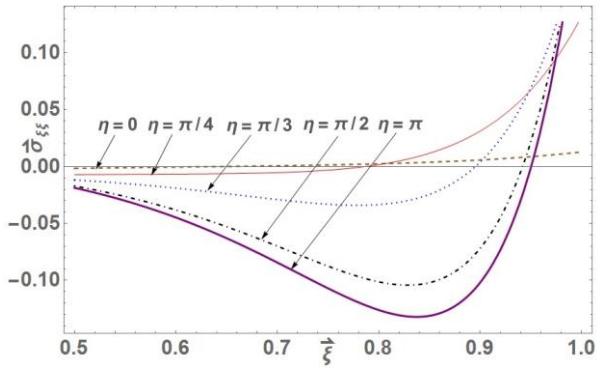

Figure 4(b) Dimensionless Radial stress along $\bar{\xi}$ for the different values of η.

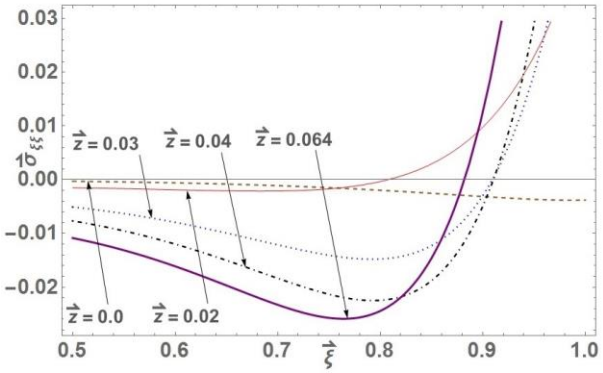

Figure 4(c) Dimensionless Radial stress along $\bar{\xi}$ for the different values of $\bar{z}$

Figure 4(a) depicts radial stress along the axial direction and attains zero at the inner boundary satisfying the condition, but increases towards outer edge even with the growth of oblique angles. This changes could be owing due to thermal expansion. Figure 4(b) illustrates that absolute value of stresses decreases at centre with the different angular angle, but increase at the outer edge. Similar radial inherent nature was found in Figure 4(c) along the radial direction for various value of *z*. Figure 4(d) shows radial stress attains maximum expansion at central part due to the accumulation of heat energy dissipated by sectional and internal heat supply which further decreases at the two extreme ends. Figures 5-6 illustrate the circumferential and shear thermal stresses.

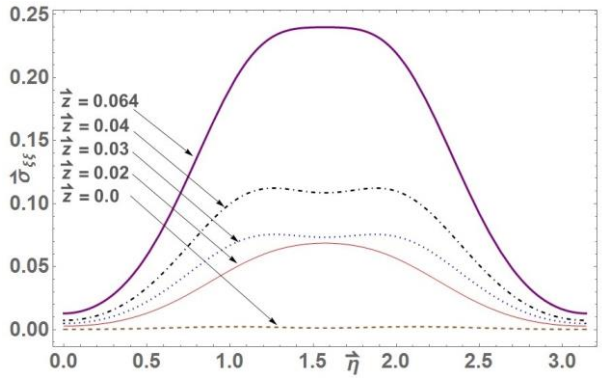

Figure 4(d) Dimensionless Radial stress along η for different values of $\bar{z}$.

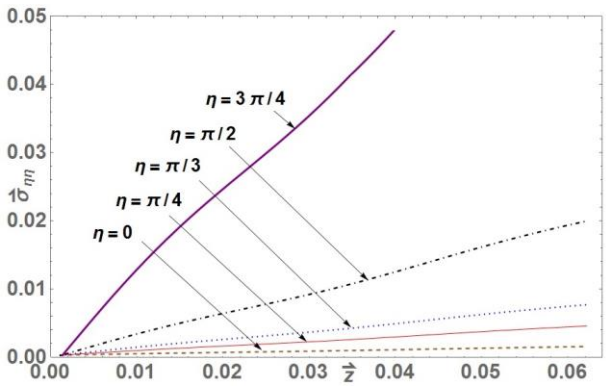

Figure 5(a) Dimensionless tangential stress along $\bar{z}$ for the different values of η.

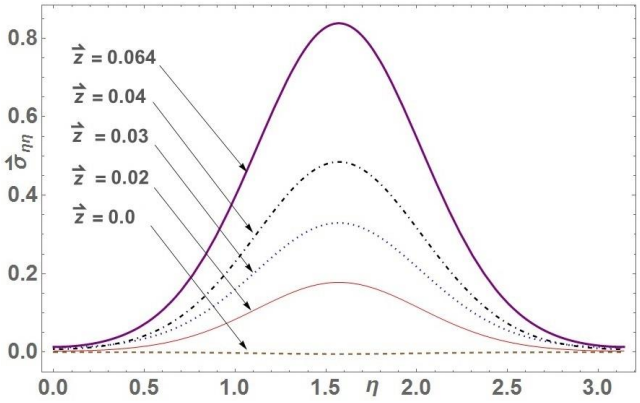

Figure 5(b) Dimensionless tangential stress along η for the various values of $\bar{z}$.

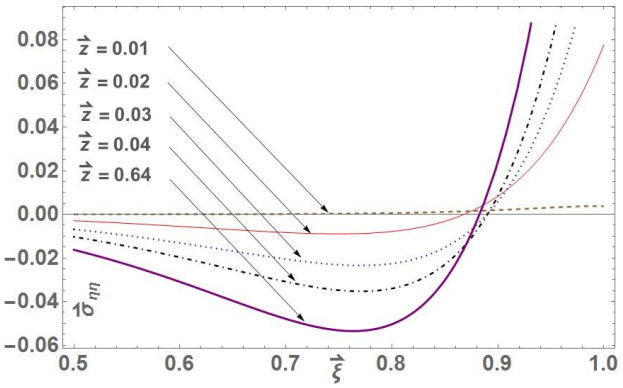

Figure 5(c) Tangential stress along $\bar{\xi}$ for the various values of $\bar{z}$.

Figure 5(a) displays that the initial stress is zero which further increase along *z* for different values of η for different values of oblique angles. It might be because of sectional heat supply. When axes were flipped, total different characteristic was found as shown in Figure 5(b), the stresses are at the maximum at the centre core and attains zero at two edges. Figure 5(c) depicts tangential stress along the radial direction for different value of *z,* and it was observed that initially stress are minimum, but as it approaches towards the outer edge, it increases gradually due to sources of heat. Finally, Figure 5(d) illustrates the thermal bending moments exhibiting its effect along the angular direction. Here moments are maximum for $M_{\xi\xi}$ and $M_{\eta\eta}$, and $M_{\xi\eta}$ is minimum at the central with both edges attaining zero's.

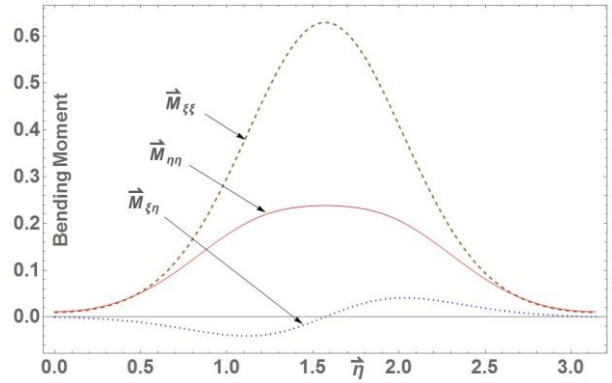

Figure 5(d) Thermal induced bending moments along η.

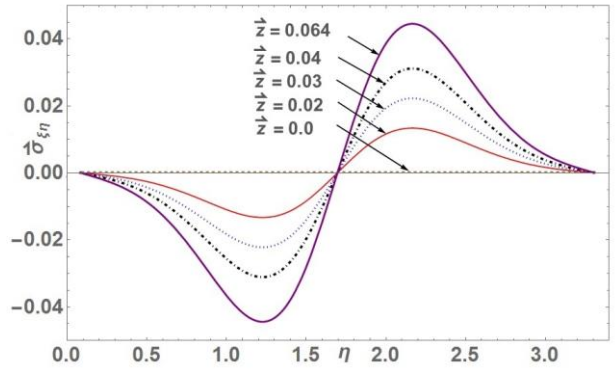

Figure 6(a) Dimensionless Shear stress along η for the different values of $\bar{z}$.

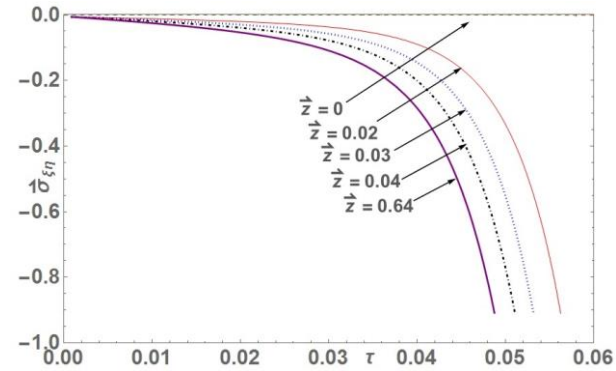

Figure 6(b) Dimensionless Shear stress along τ for the different values of $\bar{z}$.

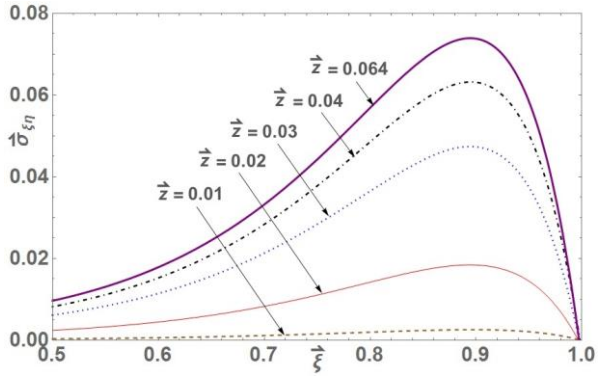

Figure 6(c) Dimensionless Shear stress along $\bar{\xi}$ for the various values of $\bar{z}$.

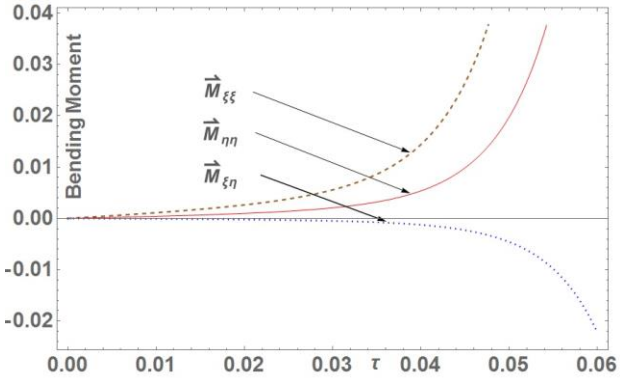

Figure 6(d) Thermally induced bending moments along τ.

Figure 6(a) shows shear stress sinusoidal in nature, and it attains zero at $0, \pi/2$ and 2π along the angular direction for different value of $\bar{z}$. Figure 6(b) depicts decreasing stress trend with time for the various values of $\bar{z}$. Figure 6(b) gradually increases towards its peak and then decreases to zero at $\bar{\xi} = b$ for the different values of $\bar{z}$. Figure 6(d) illustrates $\bar{M}_{\xi\xi}$, $\bar{M}_{\eta\eta}$ and $\bar{M}_{\xi\eta}$ variation along with time. The residual bending moments are maximum for $\bar{M}_{\xi\xi}$ and $\bar{M}_{\eta\eta}$, whereas $\bar{M}_{\xi\eta}$ indicates negative value at the outer edge.

Biswas [15] has assumed the following data in calculating the deflection at a point of a heated elliptical plate under stationary temperature based on the method devised by small deflection method as

$$\bar{\xi} = 1,\ \eta = \pi/2,\ \ell = 1,\ \bar{\xi}_0 = 0.3,\ \beta^2 = 0.01,\ c = 1,$$
$$\upsilon = 0.3,\ \alpha = 1.2\times10^{-5},\ E = 2\times10^{12},\ \bar{T}_0 = 600 \qquad (52)$$

The central deflection obtained was $\bar{\omega} = 0.018$ (approx.).

The author has applied the proposed method as given in equation (26) with same parameter above given in equation (52) and the axial deflection obtained was $\bar{\omega} = 0.0185$. The result above nearly agrees with the previously given result.

6. Conclusions

In this article, we have described the theoretical treatment of temperature distribution and the deflection in the form of ordinary and modified Mathieu functions used to determine thermal stresses by proposed new operational methods in-line with other integral transform developed by authors[16-18]. The analytical technique proposed here is relatively

straightforward and widely applicable compared to the methods proposed by other researchers. The results mentioned which were obtained while carrying out our research are illustrated as follows,

- The advantage of this approach is its generality and its mathematical power to handle different types of mechanical and thermal boundary conditions during significant deflection under thermal loading.
- The maximum tensile stress shifting from the outer surface due to maximum expansion at the outer part of the plate and its absolute value increases with radius may be attributable to heat, stress, concentration or available internal heat sources under known temperature field.
- Finally, the maximum tensile stress occurs in the circular core on the major axis as compared to elliptical central part indicates the distribution of weak heating. It might be due to insufficient penetration of heat through the elliptical inner surface.

Acknowledgements:
The author(s) are grateful to reviewer and editor for their valuable suggestion and constructive comments which resulted in revising the paper to its present form.

References:

[1] J.J. Han, N. Hasebe, "Green's function for thermal stress mixed boundary value problem of an infinite plane with an arbitrary hole under a point heat source," *J. Thermal Stresses, 25,* 1147-1160, 2002.

[2] N. Hasebe, J.J. Han, "Green's function for thin plate with elliptic hole under bending heat source," *Transactions on Modelling and Simulation, 28,* 81-90, 2001.

[3] A. Naser, "The solution of heat conduction equation with mixed boundary conditions," *J. Mathematics and Statistics, 2,* 346-350, 2006.

[4] J. Helsing, "Integral equation methods for elliptic problems with boundary conditions of mixed type," *J. Computational Physics, 228,* 8892-8907, 2009.

[5] Q.A. Dang, X.T. Mai, "Iterative method for solving a problem with mixed boundary conditions for biharmonic equation arising in fracture mechanics," *Bol. Soc. Paran. Mat., 31,* 65–78, 2013.

[6] H.R. Al Duhaim, F.D. Zaman, R.I. Nuruddeen, "Thermal stress in a half-space with mixed boundary conditions due to time dependent heat source," *IOSR J. Mathematics, 11,* 19-25, 2015.

[7] W.J. Parnell, V.-H. Nguyen, R. Assier, S. Naili, I.D. Abrahams, "Transient thermal mixed boundary value problems in the half-space," *SIAM J. Appl. Math., 76,* 845–866, 2016.

[8] R.I. Nuruddeen, F.D. Zaman, "Temperature distribution in a circular cylinder with general mixed boundary conditions," *Journal of Multidisciplinary Engineering Science and Technology, 3,* 3653-3658, 2016.

[9] S. Cheng, "Bending of an elliptic plate under a moment at the center," *Tech. Sum. Rept. No. 444,* Math. Res. Center, Univ, Wisconsin, 1963.

[10] K. Sato, "Bending of a clamped elliptical plate under the combined action of uniform lateral load and in-plane force," *Theor, and Appl. Mech, 53,* 37-47(2004).

[11] P.P. Bhad, V. Varghese, L.H. Khalsa, "Heat source problem of thermoelasticity in an elliptic plate with thermal bending moments," *J. Thermal Stresses,* doi:10.1080/01495739.2016.1211496.

[12] E. Ventsel, T. Krauthammer, Thin plates and shells-*Theory. Anal. and Appl.*, Marcel Dekker, New York, 2001.

[13] R. Kumar, N.K. Lamba, V. Varghese, "Analysis of thermoelastic disc with radiation conditions on the curved surfaces," *Materials Physics and Mechanics, 16,* 175-186 (2013).

[14] N.W. McLachlan, *Theory and Application of Mathieu function*, Oxford Univ. Press, 1947.

[15] P. Biswas, "Note on the deflection of a heated elliptic plate," *Journal of the Indian Institute of Science, 58(2),* pp. 56-61, 1976.

[16] P. Bhad, L. Khalsa, and V. Varghese, "Transient Thermoelastic Problem in a Confocal Elliptical Disc with Internal Heat Sources," *Adv. Math. Sci. Appl., 25,* pp. 43–61, 2016.

[17] P. Bhad, L. Khalsa, and V. Varghese, "Thermoelastic theories on elliptical profile objects: An overview & prospective," *Int. J. Adv. Appl. Math. and Mech., 4(2),* pp.12-20, 2016.

[18] P. Bhad, L. Khalsa, and V. Varghese, "Thermoelastic-induced vibrations on an elliptical disk with internal heat sources," *Journal of Thermal Stresses,* doi:10.1080/01495739.2016.1254075.